Available online at www.sciencedirect.com
SCIENCE DIRECT
Journal of Molecular Structure 782 (2006) 191–199
Journal of MOLECULAR STRUCTURE
www.elsevier.com/locate/molstruc

Intramolecular hydrogen bonding in 2-nitromalonaldehyde: Infrared spectrum and quantum chemical calculations

S.F. Tayyari[a,*], Z. Moosavi-Tekyeh[a], M. Zahedi-Tabrizi[b], H. Eshghi[a], J.S. Emampour[a], H. Rahemi[c], M. Hassanpour[d]

[a]*Chemistry Department, Ferdowsi University, Mashhad 91774-1436, Iran.*
[b]*Chemistry Department, Alzahra University, Tehran 1993891167, Iran.*
[c]*Chemistry Department, Urmia University, Urmia57159-165, Iran.*
[d]*Chemistry Department, Khayyam Higher Education Center, Mashhad 91897, Iran*

Received 28 May 2005; revised 9 August 2005; accepted 15 August 2005
Available online 21 September 2005

Abstract

2-Nitromalonaldehyde (NO_2MA), a simple compound to study the intramolecular hydrogen bond, has been synthesized and deuterated at the enolated proton. Molecular structure and vibrational frequencies of NO_2MA have been investigated by means of density functional theory (DFT) calculations. The geometrical parameters obtained in the B3LYP level using 6-31G**, 6-311G**, and 6-311++G** basis sets and compared with the corresponding parameters of malonaldehyde (MA). Frequencies calculated at B3LYP level using the 6-311G** and 6-311++G** basis sets are in good agreement with the corresponding experimental results for light and deuterated compounds in CCl_4/CS_2 solution. The percentage of deviation of the bond lengths and bond angles was used to give a picture of the normal modes, and serves as a basis for the assignment of the wavenumbers.

Theoretical calculations show that the hydrogen bond strength of NO_2MA is slightly stronger than that of MA, which is in agreement with the spectroscopic results. The observed νOH/νOD and γOH/γOD appears at about 2880/2100 and 911/695 cm^{-1}, respectively, are consistent with the calculated geometry and proton chemical shift results.

To investigate the effect of NO_2 group on the hydrogen bond strength, the charge distributions, steric effects, and electron delocalization in NO_2MA and MA were studied by the Natural Bond Orbital (NBO) method for optimized model compounds at B3LYP/6-311++G** level of theory. The results of NBO analysis indicate that the electron-withdrawing effect of NO_2 group decreases the hydrogen bond strength, but the steric and resonance effects increase the strength of the bond.

Keywords: 2-Nitromalonaldehyde; Intramolecular hydrogen bond; Infrared spectra; Steric effect; Natural Bond Orbital theory.

1. Introduction

The *cis*-enol form of β-diketones is stabilized by a strong intramolecular hydrogen bond [1–4], which belongs to the class of the Resonance Assisted Hydrogen Bonds (RAHB) [5]. The strength of the bridge could be more or less modified by the presence of substituents, which, depending on the nature and position of the substituents, different effects could be induced to the π-electron delocalization in the enol ring [6,7].

The vibrational spectra of these compounds have been the subject of numerous investigations, which support the existence of a strong intramolecular hydrogen bond of chelating nature in the enol form of β-diketones [8–15]. This hydrogen bond formation leads to an enhancement of the resonance conjugation of the π-electrons, which causes a marked tendency for equalization of the bond orders of the valence bonds in the resulting six-member chelated ring. Therefore, it seems that any parameter that affects the electron density of the chelated ring will change the hydrogen bond strength. Alkyl or aryl substituents at the α-position of β-diketones cause a dramatic decrease in the enol content, which becomes very low for bulky substituents, but enhances the hydrogen bond strength [16–20].

* Corresponding author. Tel.: +985118780216; fax: +985118438032.
E-mail address: sftayyari@yahoo.com (S.F. Tayyari).

0022-2860/$ - see front matter © 2005 Elsevier B.V. All rights reserved.
doi:10.1016/j.molstruc.2005.08.012

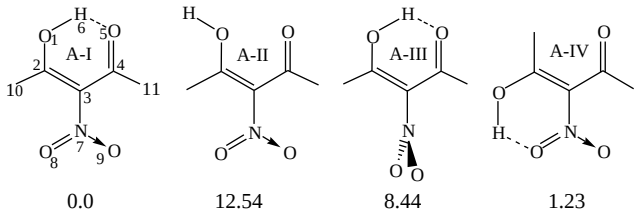

Fig. 1. Schematic representation for the two stable structures of NO_2MA, A-I, and A-IV, open stucture, A-II, and rotated NO_2 group, A-III and their relative energies in kcal/mol.

NO_2MA can have two types of intramolecular hydrogen bonded conformations that are stabilized by π-delocalization, one between OH group with the carbonyl group, A-I, and the other between OH group with one of the NO_2 oxygen atoms [7], A-IV in Fig. 1. On the other hand, MA and its derivatives form intermolecular hydrogen bond in the solid state [21–23].

The main intention of this study was to improve the understanding of the factors that govern the intramolecular hydrogen bond strength in the cis enol form of β-diketones. In the present paper: (1) we recorded the FT-IR spectra of NO_2MA and its deuterated analogue in CCl_4 solution. Based on DFT calculation at B3LYP/6-311++G** level of theory and frequency changes upon deuteration, a complete assignment of vibrational frequencies was performed and the results were compared with those of MA. (2) Comparison of NO_2MA and MA geometrical parameters, charge distribution, steric effects, and resonance energies give a clear understanding of substitution effects of NO_2 group on the structure and hydrogen bond strength of the system.

2. Experimental

2.1. Preparation

2.1.1. Sodium 2-nitromalonaldehyde monohydrate ($NaNO_2MA \cdot H_2O$)

This compound was prepared as reddish-brown crystals by dropwise adding a solution of Mucobromic acid [24] in ethanol to an aqueous solution of sodium nitrite at 54 ± 1 °C. As small quantities of HCN are evolved in this reaction, appropriate precautions were taken.

2.1.2. 2-Nitromalonaldehyde

Because of unstability of NO_2MA in aqueous solutions, it was obtained by bubbling HCl to a suspension of $NaNO_2$-MA in dry CCl_4. HCl was prepared by adding dropwise H_2SO_4 to NaCl and then passing the gas over P_2O_5 for further drying. By bubbling dry HCl gas through the suspension, a clear solution with precipitated NaCl was obtained. CCl_4 solution was decanted from NaCl and distilled by rotary evaporator. NO_2MA was obtained as white needles in 75% yield mp 50–51 °C, ^1H NMR ($CDCl_3$): δ 9.5 (s, 1H, CH) and δ 13.75 (s, 1H, OH).

2.1.3. Deuterated NO_2MA (DNO_2MA)

Deuterated NO_2MA was prepared with the same procedure reported for NO_2MA using D_2SO_4 for generation of DCl as described for HCl, then passing gaseous DCl through suspension of $NaNO_2MA$ in CCl_4 to obtain DNO_2MA. The resulted solution, after separation of NaCl, was directly used to obtain the IR spectrum of deuterated NO_2MA in solution.

2.2. Instrumentation

The mid-IR spectra of NO_2MA and its related compounds were recorded by using Bomem MB-154 Fourier Transform Spectrophotometer in the region 500–4000 cm^{-1} in KBr pellet and in CCl_4/CS_2 solution. The spectrum was collected with a resolution of 2 cm^{-1} by coadding the results of 16 scans.

The Far-IR spectra in the region 600–50 cm^{-1} were obtained using a Thermo Nicolet NEXUS 870 FT-IR spectrometer equipped with DTGS/polyethylene detector and a solid substrate beam splitter. The spectra were collected with a resolution of 4 cm^{-1} by coadding the results of 128 scans.

The NMR spectra were obtained on a FT-NMR, Brucker Aspect 3000 spectrometer at 100 MHZ frequency using 2 mol% solutions in $CDCl_3$ at 22 °C.

3. Theoretical methods

Geometrical calculations were performed using Gaussian 03 version B05 [25] and NBO 5.0 [26] programs. Geometry of cis enol form of NO_2MA, A-I in Fig. 1, and MA are fully optimized with hybrid density functional B3LYP [27,28] using 6-31G**, 6-311G**, and 6-311++G** basis sets. Frequencies calculations were performed at B3LYP level of theory using 6-311G** and 6-311++G** basis sets. Orbital population and Wiberg bond orders [29] were calculated with NBO 3.0 program implemented in Gaussian 03. Natural steric analysis [30,31] and second order interaction energies (E^2) [32] were performed at the B3LYP/6-311++G** level using NBO 5.0 program, which applied the wavefunction information file generated by the earlier version of NBO (3.0).

To show the effect of hydrogen bond formation on the π-electron delocalization and charge distribution, the open structure, A-II in Fig. 1, was also fully optimized at the B3LYP/6-311++G** level of theory. To understand the effect of resonance between NO_2 group and enol ring on the hydrogen bond strength and π-delocalization, the NO_2 group was rotated by 90° about the C-N bond, A-III in Fig. 1, and its geometry was fully optimized, with CCNO

dihedral angle constrain, at the B3LYP/6-311++G** level of theory.

The assignment of the experimental frequencies are based on the observed band frequencies and intensity changes in the infrared spectrum of the deuterated species confirmed by establishing one to one correlation between observed and theoretically calculated frequencies.

4. Results and discussion

4.1. Molecular geometry

All possible single molecular structures of NO_2MA have been considered by Buemi and Zuccurello [7], which the geometrical parameters were determined at B3LYP/6-31G** level of theory. We only considered the most stable structure, A-I, and its open structure, A-II in Fig. 1.

The full-optimized geometries of cis-enol form of A-I, A-II, A-III, and MA and the reported experimental structure of MA [33] are compared in Table 1.

In all calculations for A-I and A-II the oxygen atoms of NO_2 group lie in the plane of enol ring and, therefore, a significant conjugation between the NO_2 group and the enol ring is to be expected. The planarity of the molecule is in agreement with the microwave experimental data [34].

As it is obvious from Table 1, the main effect of NO_2 substitution is shortening of the O···O distance and lengthening of the O–H bond length in comparison with the corresponding values for MA. The calculated O···O and O···H distances in NO_2MA are 0.02–0.028 and 0.027–0.036 Å, respectively, shorter than those in MA. These results suggest a stronger hydrogen bond in NO_2MA than that in MA. On the other hand, by rotating the NO_2 group by 90° about C–N bond, A-III, the O···O distance increases by about 0.05 Å (see Table 1). Two factors could be considered to account for this hydrogen bond weakening, lower π-electron conjugation between enol ring and NO_2 group and less steric effects between the NO_2 group and the rest of the molecule.

Table 1 also shows that upon nitro substitution on α-position both C–C and C=C bond lengths are increased, whereas C–O and C=O bond lengths are decreased. The bond length increment in C=C could be attributed to the π-electron delocalization through NO_2–C=C fragment of the molecule, which reduces its double bond character. The bond length increment in C–C could be attributed to reduced electron delocalization in O=C–C fragment of the chelated ring, which increases its single bond character. This interpretation also accounts for shortening of C=O bond length. Reduction in the C–O bond length could be well described by considering increased π-electron delocalization in the C–O side due to the effect of the NO_2 group. The effect of the nitro group on the π-delocalization in the chelated ring could also be explained in the terms of the Gilli's symmetry coordinates [35] q_1 ($d_{C-C}-d_{C=C}$), q_2 ($d_{C-O}-d_{C=O}$), $Q=q_1+q_2$ (see Table 1). By comparing these coordinates for NO_2MA and MA, one can deduce that there is more bond equalization, in NO_2 substituted MA than in MA itself. These coordinates considerably increase in A-II, which indicate the effect of hydrogen bond formation on the bond equalization in the enol ring.

Table 1
Selected geometrical parameters of NO_2MA and MA calculated at B3LYP level[a]

	NO_2MA					MA			Exp.[33]
	A-I			A-II	A-III				
	B1	B2	B3	B1	B1	B1	B2	B3	
Bond lengths (Å)									
O–H	1.004	1.014	1.008	0.964	0.994	0.997	1.007	1.000	(0.969)[b]
O···H	1.664	1.614	1.635	–	1.738	1.7	1.641	1.671	1.68
O···O	2.559	2.534	2.543	2.807	2.61	2.587	2.554	2.57	2.553
C2–O1	1.303	1.304	1.301	1.324	1.314	1.319	1.319	1.317	1.32
C4=O5	1.234	1.241	1.233	1.21	1.231	1.238	1.245	1.237	1.234
C2=C3	1.374	1.378	1.371	1.356	1.36	1.364	1.368	1.361	1.348
C3–C4	1.448	1.445	1.443	1.48	1.442	1.438	1.437	1.434	1.454
C4–H11	1.096	1.098	1.094	1.101	1.086	1.103	1.105	1.101	1.089
C2–H10	1.084	1.086	1.089	1.085	1.101	1.086	1.089	1.085	1.091
Bond angles (°)									
O1–C2–C3	122.8	122.4	122.5	122.8	124.2	124.2	123.9	124.0	123.0
C3–C4–O5	120.8	120.9	121.1	123.1	121.3	123.3	123.4	123.5	124.5
C2–C3–C4	121.0	120.5	120.8	126.5	122.4	119.7	118.9	119.5	119.4
q_1	0.069	0.063	0.068	0.114	0.083	0.081	0.074	0.08	0.086
q_2	0.074	0.067	0.072	0.146	0.082	0.074	0.069	0.073	0.106
Q	0.143	0.13	0.14	0.26	0.165	0.155	0.143	0.153	0.192

[a] B1, B2, and B3 stands for 6-311++G**, 6-311G**, and 6-31G**, respectively.
[b] Assumed value.

Table 2
Selected Wiberg bond order of NO_2MA and MA calculated at B3LYP/6-311++G** level

Bond	A-I	A-II	A-III	MA
O1–H6	0.6255	0.7491	0.6481	0.6406
C2–O1	1.2578	1.1549	1.2054	1.1899
C2–C3	1.4825	1.5898	1.561	1.6027
C3–C4	1.1504	1.0595	1.161	1.2058
C4–O5	1.6756	1.8239	1.6784	1.6446
C3–N7	0.9647	0.9522	0.8889	–
N7–O8	1.4869	1.4778	1.5247	–
N7–O9	1.4838	1.4973	1.5247	–

Table 3
Selected natural charges (e) for the optimized rotamers of NO_2MA and MA at B3LYP/6-311++G** level

Atom	A-I	A-II	A-III	MA
O1	−0.6	−0.593	−0.616	−0.642
O5	−0.588	−0.508	−0.584	−0.618
C3	−0.159	−0.118	−0.144	−0.464
C2	0.345	0.29	0.311	0.305
C4	0.39	0.379	0.385	0.381
H6	0.51	0.487	0.511	0.507

4.2. NBO analysis

4.2.1. Bond order

The calculated Wiberg bond orders [29] for A-I, A-II, A-III, and MA are collected in Table 2.

Table 2 shows that the bond orders of C=C and C–O considerably and C–C and C=O slightly change from MA to A-I. These changes are in line with the bond lengths changes discussed in the last section and confirm significant increase in the π-electron delocalization through NO_2–C=C–O fragment of A-I molecule. Slightly increase in the C=O bond order and decrease in the C–C bond order are also in agreement with reduction of electron delocalization in the O=C–C fragment of the chelated ring.

Rotation of NO_2 group by 90° considerably affects the bond orders of C=C, C–O, C–N, and N–O, which also confirms contribution of NO_2 group in O=N–C=C–O fragment of the molecule when it is coplanar with the enol ring. Comparison between bond orders in A-I and A-II clears the significant effect of intramolecular hydrogen bond formation on the π-electron delocalization in the enolated ring.

It is noteworthy that the bond order of O–H could be correlated with the O···O distance; the O–H bond order increases by increasing the O···O distance.

4.2.2. Charge analysis

The charge distribution calculated by the NBO method for optimized geometries of A-I, A-II, A-III, and MA are tabulated in Table 3. According to this Table, the electron withdrawing effect of the NO_2 group considerably reduces the electronic charge over the enolated ring in A-I and A-III conformers, compared with MA. Weaker intramolecular hydrogen bond in A-III, with least steric and resonance effects, clearly explains the electron withdrawing effect on weakening of hydrogen bond in these systems. Therefore, to explore the reasons for stronger hydrogen bond in NO_2MA compared with that in MA, resonance and steric effects should be considered.

4.2.3. Electron delocalization

Delocalization of electron density between occupied Lewis-type (bond or lone pair) NBO orbitals and formally unoccupied (antibond or Rydberg) non-Lewis NBO orbitals corresponds to a stabilizing donor–acceptor interaction. The energy of this interaction can be estimated by the second order perturbation theory [32].

Table 4 lists the calculated second order interaction energies (E^2) between the donor–acceptor orbitals in A-I, A-II, A-III, and MA. The most important interaction energy, related to the resonance in the enol ring, is electron donation from LP(2)O1 to the antibonding acceptor π*(C2–C3) orbital in the NO_2MA (54.4 kcal/mol). The contribution of this interaction in MA is reduced by about 7 kcal/mol, which indicates the effect of NO_2 group on the resonance in the enolated ring. An energy decrease of about 11 kcal/mol in this interaction along with a decrease of about 24, 10, and 5 kcal/mol in the LP(2)O5 → σ*(O1–H6), π(C2–C3) → π*(C4–O5), and LP(1)O1 → σ*(C2–C3), respectively, in

Table 4
Selected second-order perturbation energies $E^{(2)}$ (donor → acceptor)[a]

Donor	Type	Acceptor	type	A-I	A-II	A-III	MA
C2–C3	π	C4–O5	π*	28.8	18.6	29.0	30.7
C2–C3	π	C2–C3	π*	7.8	5.7	5.7	5.9
O5	CR	C4	RY*	5.3	5.8	5.2	5.4
O1	LP(1)	C2–C3	σ*	5.6	0.7	5.5	5.7
O1	LP(2)	C2–C3	π*	54.4	43.5	49.4	47.3
O5	LP(1)	C4	RY*	9.9	13.5	10.8	10.8
O5	LP(2)	O1–H6	σ*	24.0	–	16.9	20.6
O5	LP(2)	C3–C4	σ*	12.2	20.5	13.6	11.2
O5	LP(2)	C4–H11	σ*	16.8	20.4	18.6	18.3
C2–C3	π	N7–O9	π*	28.9	24.7	8.1	–

[a] Energy in kcal/mol.

Table 5
Important pairwise steric exchange energies ΔE (i,j) (kcal/mol) interactions between NLMOs i,j

NLMO (i)		NLMO (j)		A-I	A-II	A-III	MA
O1–H6	σ	O5	LP (2)	17.43	–	13.09	16
C2–C3	π	N7–O9	π	7.95	7.56	–	–
C2–C3	π	O1	LP (2)	15.1	15.4	15.21	16
C2–H10	σ	O1	LP (1)	2.39	8.44	2.48	2.3
C4–H11	σ	O9	LP (2)	2.27	3.09	–	–
C2–H10	σ	O8	LP (2)	2.36	3.60	–	–

A-II compared to those in A-I indicate the hydrogen bond formation effect on the π-electron delocalization in the enol ring. These interactions are only slightly compensated by LP(2)O5 → σ*(C3–C4) with a value of about 8 kcal/mol. The relatively high interaction energy of π(C2–C3) → π*(N7–O9) in A-I, 28.9 kcal/mol, compared with that in A-III, 8.1 kcal/mol, clearly indicates the increase of π-electron delocalization through NO_2–C=C fragment of the molecule in A-I and considerably reduction in electron delocalization due to the removing of NO_2 group from the plane of enol ring in A-III.

4.2.4. Steric effect

The most important pairwise steric exchange energies, $\Delta E(i,j)$, interactions between NLMOs are listed in Table 5. According to this Table, the strong steric exchange energy between π(C2–C3) and π(N7–O9) in A-I and A-II, 7.95 and 7.56 kcal/mol, respectively, disappears in A-III rotamer. There are also some steric effects between σ(C4–H11) and σ(C2–H10) with electron lone pairs of nitro oxygen atoms, which are absent in the case of A-III conformation. These steric interactions are responsible for pushing oxygen atoms of the enol ring, Which results in shorter O···O distance. Longer O···O distance in A-II compared with that in A-I results in a strong steric interaction between σ(C2–H10) and LP(1)O1 (8.44 kcal/mol), which the corresponding interaction in A-I and A-III is considerably weaker (2.4–2.5 kcal/mol).

5. Vibrational analysis

Since it has been shown that MA derivatives exist as the cis enol form in solutions and trans enol form in the solid state, which in the latter the molecule stabilized through an intermolecular hydrogen bond [21–23], therefore, we only considered the infrared spectrum of NO_2MA in solution.

The IR spectra of NO_2MA and its deuterated analogous in solution are shown in Figs. 2 and 3, respectively. Lorentzian function has been utilized for the deconvolution of infrared spectrum of NO_2MA in the 3500–2000 region as shown in Fig. 4. The calculated and experimental vibrational frequencies for NO_2MA and its deuterated analogue are tabulated in Tables 6 and 7, respectively. The Cartesian representation of the normal modes, in the absence of the potential energy distribution (PED), permits, in the quantum mechanic ab initio DFT method, to study the distorted geometry of each mode [36].

The assignment of the experimental frequencies are based on the observed band frequencies and intensity changes in the infrared of the deuterated species confirmed by establishing one to one correlation between observed and theoretically calculated frequencies.

5.1. Vibrational assignment of NO_2MA in solution

5.1.1. The CH and OH stretching region

Deconvolution of IR spectrum of NO_2MA in CCl_4 in 3500–2000 cm^{-1} region, Fig. 4, exhibits a broad band with

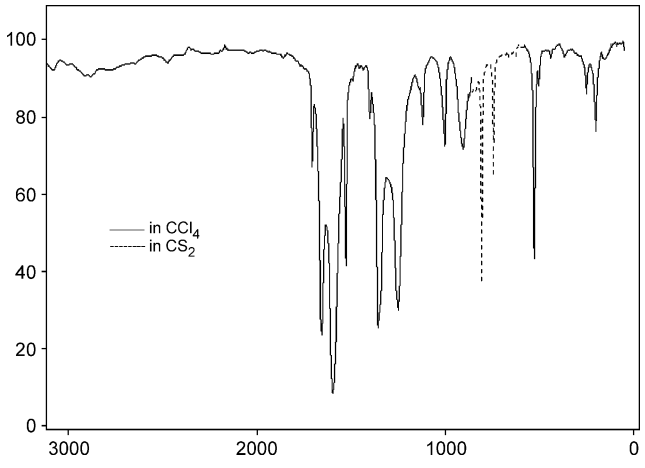

Fig. 2. IR spectrum of NO_2MA in CCl_4/CCl_4.

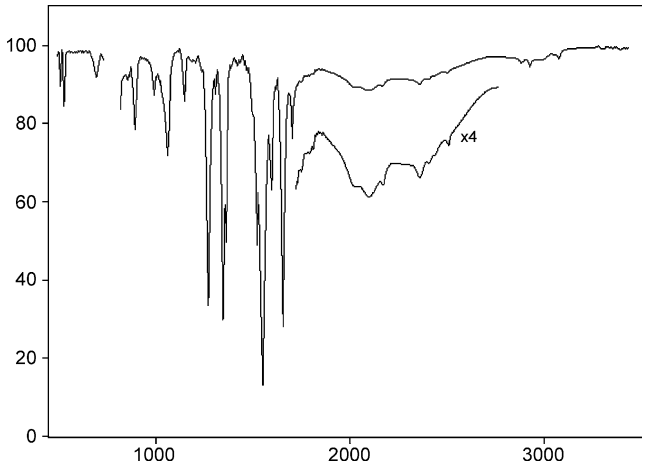

Fig. 3. IR spectrum of D-NO_2MA in CCl_4.

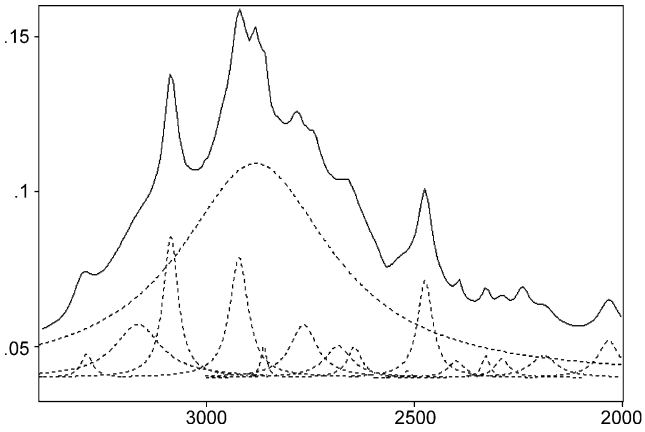

Fig. 4. The deconvoluted IR spectrum of NO_2MA in CCl_4 in the νOH region.

several sharp bands in this region. The two strongest bands at 3085 and 2920 cm^{-1} are attributed to the vinylic and aldehydic CH stretching modes. According to the calculation results these two bands are somewhat coupled to the OH stretching modes and upon deuteration considerably loose their intensity. The broad bandwidth at half-height, $\nu_{1/2}$, of about 440 cm^{-1} centered at 2880 cm^{-1} is assigned to OH stretching. The weakness and broadness of this band is the characteristic of the enol form of β-diketones and appears at 3000–2600 cm^{-1} [8,9]. It has been shown that increasing the hydrogen bond strength decreases the intensity of this band and increases its bandwidth [9]. Upon deuteration, this band disappears and a new band with considerably reduced bandwidth, $\nu_{1/2} \approx 150\ cm^{-1}$, appears at about 2100 cm^{-1}. It has been shown for several enolated β-diketones that the $\nu_{1/2}OH/\nu_{1/2}OD$ is greater than 2. This great reduction in bandwidth is attributed to existence of a double minimum potential function for the proton movement in these hydrogen-bonded systems [9]. This result is consistent with the microwave results, which indicates a double minimum potential for NO_2MA, with a tunneling frequency of $35 \pm 15\ cm^{-1}$, [34]. ν_{OH}/ν_{OD} ratio of about 1.37 for the titled compound suggests an intramolecular hydrogen bond with moderate strength, with a hydrogen bond strength of about that of trifluoro-acetylacetone [9]. The position of νOH in MA is not very clear, but the corresponding band in deuterated MA appears at 2140 cm^{-1} [13], which is in agreement with the calculated results.

Table 6
Fundamental band assignment of NO_2MA[a]

No.	Theoretical					Exp.		Assignment
	A		B					
	F	I	F	I	R	F	I	
1 A′	3207	3	3224	1	69	3083	3	νCHν(73) + νOH(13)
2	3084	49	3091	2	100	2920	2	νCHa(55) + νOH(22) + νCHν(10)
3	3063	15	2937	69	42	2880	vbr	νOH(59) + νCHa(21) + νCHν(10)
4	1700	59	1719	51	8	1657	60	νC=O (15) + νC=C(10) + δCH(20)
5	1629	100	1664	100	21	1598	100	νaC–C=C(18) + δOH(19) + νaNO_2(15)
6	1573	21	1619	14	18	1525	57	νaNO_2(31) + δOH(14) + δCHν(11)
7	1431	0	1450	0	2	–	–	νC–C(11) + δCH(21) + νaNO_2(10) + νC=C(8)
8	1393	8	1419	15	71	1382	sh	δOH(25) + νsC–C=C–O(16) + νsC=C–C=O(19)
9	1381	3	1405	38	90	1358	32	δCHa(27) + νC–O(10) + νsNO_2(16) + νC–N(12)
10	1367	78	1380	42	1	1348	31	νsNO_2(21) + δCH(22) + νC–N(10)
11	1284	56	1294	42	0	1250	60	δOH(21) + νC–O(15) + δCHν(27)
12	1137	9	1159	8	6	1120	8	νC–N(15) + δCCC(12) + νC–C(10)
13	938	5	975	8	3	927	2	νsC=C–C(17) + Δ(36)
14	828	8	820	8	3	808*	30	δNO_2(47) + Δ(27)
15	532	6	537	7	0	528	26	Δ(33) + ρNO_2(19)
16	507	0	515	0	11	506	3	Δ(36) + δCH(18) + ρNO_2(18)
17	441	0	447	0	4	441	1	νC–NO_2(20) + δC=C–O(11)
18	283	2	287	2	1	287	sh, br	νO···O(62)
19	252	1	254	1	0	252	3	δC–NO_2(30) + νO···O(20)
20 A″	1060	13	1080	19	0	1012	5	γCH ν(38) + γOH(26) + γCHa(17)
21	1029	3	1038	1	5	1004	11	γCHa(37) + γOH(19)
22	936	12	984	5	24	911	14,br	γOH(42) + γCH ν(20)
23	728	2	752	3	1	744*	15	ωNO_2(49)
24	369	0	378	0	1	369	1	Γ(51) + γCH(35)
25	292	1	313	1	1	[287]	–	Γ(32) + γCH(30)
26	196	3	206	3	1	200	6	γNO_2(70)
27	55	0	70	0	0			τNO_2(72)

[a] I, IR relative intensity, *R*=Raman relative intensity; *F*=frequency in cm^{-1}, A and B are stand for calculation at B3LYP/6-311 + + G** and B3LYP/6-311G** level of theory, respectively; sh, shoulder; w, weak; s, strong; br, broad. ( ), band overlapped contributions less than 5% are omitted and percent of contributions are given in parenthesis.

Table 7
Fundamental band assignment of D-NO_2MA. Frequencies are in cm^{-1}

No.	Theoretical					Exp.		Assignment
	A		B					
	F	I	F	I	R	F	I	
1 A′	3204	0	3222	0	58	3078	2	νCHν(84)
2	3066	2	3090	5	75	2928	4	νCHa(90)
3	2254	41	2154	66	10	2100	w,vbr	νOD(77)
4	1699	56	1717	74	6	1655	67	νC=O(15)+νC=C(9)+ δCHa(20)+ νC-O(6)+ νC-C(5)
5	1597	100	1640	100	6	1551	100	$\nu_a NO_2$(31)+ νC=C(8)+ νC=O(7)+νC–C(8)
6	1531	9	1553	31	43	1498	9	νC=O(11)+ νC-O(10)+ δOD(9)+ δCHν(7)
7	1428	0	1447	2	6	1400	2	νC-C(11)+ δCH(21)+ $\nu a NO_2$(10)+νC=C(8)
9	1381	3	1408	73	100	1363	12	νCN(12)+ νC–O(8)+δCHa(22)+ $\nu s NO_2$(13)
8	1367	78	1383	47	0	1348	60	$\nu s NO_2$(24)+ δCH(24)+ νC-N(11)
10	1309	35	1317	27	3	1271	54	δCH(44)+ νC-O(14)+δO-D(6)+νC=C(5)
11	1172	3	1194	6	1	1149	8	νC-N(12)+ δOD(16)+ δCCC(11)
12	1078	25	1099	37	5	1061	16	δOD(20)+ δCHν(15)+νC-C(11)+νC-O(8)
13	909	7	920	9	19	894	13	δOD(19)+ νC=C(9)+ νC=O(15)+νC-C(5)
14	819	6	813	5	1	* [a]		δNO_2(41)+ δOD(9)+δCCC(10)
15	530	6	534	9	1	525	21	Δ(29)+ ρNO_2(29)
16	502	1	511	0	8	507	17	Δ(35)+ ρNO_2(14)
17	434	0	440	1	3	[b]		νCN(19)+Δ(41)
18	276	2	278	3	1	[b]		νO···O(84)
19	250	1	252	1	0	[b]		δC–NO_2(34)+νO···O(30)
20 A″	1040	0	1044	1	4	–	-	γCHν(44)+ γCHa(42)
21	1006	1	1014	1	2	988	7	γCHa(26)+ γCHν(31)
22	734	4	752	9	0	(695)	14	γOD(37)+ γCN(30)
23	724	13	768	22	1	(695)	(14)	γOD(40)+ γCN(28)+ γCH(17)
24	358	0	368	0	1	[b]		Γ(52)+ γCH(36)
25	292	1	313	1	1	[b]		Γ(40)+γCH(36)
26	194	3	204	4	1	[b]		γNO_2(42)
27	55	0	70	0	0	[b]		τNO_2(72)

See footnote of Table 6.
[a] Solvent overlapped.
[b] Not measured.

5.1.2. Below 1800 cm^{-1} region

In addition to the symmetric and asymmetric NO_2 stretching and in-plane CH bending modes, five bands are expected to be observed in this region in relation to the enol ring motions due to the C=O, C–O, C=C, C–C stretching, and the OH bending modes.

A relatively weak band is observed at 1710 cm^{-1}, which upon deuteration neither its position nor its intensity changes. Assigning of this band to any normal mode corresponding to the *cis* enol form, A-I, is unlikely. This band could be assigned to the C=O stretching of the carbonyl group in another rotamer, which is engaged in an intramolecular hydrogen bonding between the hydroxyl group and one of the oxygen atoms of the nitro group (A-IV, Fig. 1). Buemi and Zuccurello, according to an ab initio calculations [7], suggested the presence of this conformer up to 10 percent, although, the weakness of 1710 cm^{-1} band indicates much lower content of this rotamer, if exists any. This is in agreement with the NMR results, which does not show any measurable content of other forms.

The two very strong bands at 1657 and 1598 cm^{-1} in the infrared spectrum of NO_2MA, based on normal mode analysis, assigned to the asymmetric and symmetric C=C–C=O stretching, respectively, which the latter is mixed with the OH in-plane bending and asymmetric NO_2 stretching motions. The corresponding bands in the parent molecule, MA, appear at 1655 and 1593 cm^{-1}. Upon deuteration the former shifts only 2 cm^{-1} and the latter shifts 100 cm^{-1} towards lower frequencies. This frequency shifts are in well agreement with the results of the DFT calculations. The coupling between symmetric C=C–C=O stretching and OH bending is the main reason of this large red shift of the 1598 cm^{-1} band. Although, a small part of this large frequency shift caused by the coupling of this band with the $\nu_{as}NO_2$, which in the light compound appears below and in the deuterated case appears at above of the band. A blue shift of about 26 cm^{-1} in $\nu_{as}NO_2$ upon deuteration confirms this explanation. Another feature of this band is its Raman intensity change upon deuteration, which is also characteristic of the enolated β-diketones [8,9,12–15]. According to the DFT calculations, the Raman intensity of

this band greatly increases upon deuteration. This behavior is caused by decoupling from OD bending and increasing the C=C and C=O character of this mode.

The strong bands at 1525 and 1358 cm^{-1} are assigned to the asymmetric and symmetric NO_2 stretching vibrations, respectively. In aliphatic compounds $\nu_{as}NO_2$ and νsNO_2 appear at 1556–1545 cm^{-1} and 1390–1355 cm^{-1}, respectively, and by conjugation with aromatic groups both of them show red shift [37]. With increasing the electron withdrawing ability of the substituted groups the frequency of the asymmetric NO_2 stretching increases [38,39]. Therefore, the relatively low frequencies of these two bands in NO_2MA could be attributed to the conjugation between the NO_2 group and enol ring. Therefore, it could be concluded that the enolated ring has a character near to that of aromatic rings and acts as electron donor to the NO_2 group.

The band at 1250 cm^{-1}, which upon deuteration disappears, assigned to the OH in-plane bending mode. This band is coupled with C–O stretching and C–H in-plane bending modes and upon deuteration disappears and a new band appears at 1061 cm^{-1}, which is mainly δOD.

Two bands at 1012, 1004 cm^{-1}, according to the calculations, are mainly arisen from C–H out-of-plane bending modes and are strongly coupled to the OH out-of-plane bending mode. The broad band at about 910 cm^{-1}, which disappears upon deuteration, is assigned to the γOH, which is strongly coupled to the γCH's. Deconvolution of the infrared spectrum of NO_2MA in CS_2 solution in this region gives a broad band centered at about 906 cm^{-1} with a bandwidth at half height of about 40 cm^{-1}. The broadness of the band and its disappearing upon deuteration confirm the assignment. The corresponding band in MA appears at 873 cm^{-1}, which indicates a weaker hydrogen bond in MA compared with that in NO_2MA. In deuterated NO_2MA and MA the OD out-of-plane bending appears at 695 and 670 cm^{-1}, respectively. These results also confirm the stronger intramolecular hydrogen bond in NO_2MA than that in MA.

It is noteworthy that the γOH/γOD ratio of about 1.31 for NO_2MA is considerably lower than that observed for the enol form of other β-diketones, 1.33-1.38 [9]. The low value of this ratio could be attributed to the coupling between γCH, 1004 cm^{-1}, and γOH, 910 cm^{-1}. This coupling causes the former moves towards higher frequencies and the latter moves towards lower frequencies. Upon deuteration, this coupling removes and the band at 1004 cm^{-1} moves to 988 cm^{-1}, which is correctly predicted by the calculations.

The weak band at 744 cm^{-1} is assigned to the NO_2 wagging. The strong band at 528 cm^{-1}, which is unaffected upon deuteration, according to the calculations, is assigned to one of the in-plane ring deformations.

Another very important band in this region is due to the O···O stretching, which appears at 287 cm^{-1}.

The strong band at 200 cm^{-1}, according to our calculation, is due to the NO_2 out-of-plane rocking mode.

6. Conclusion

We have tried to analyze the vibrational spectra of nitromalonaldehyde and its deuterated analogues by establishing one to one correlations between theoretically calculated frequencies at fairly high level with the experimental results. From the OD stretching and OH/OD out-of-plane bending modes a stronger intramolecular hydrogen bond in NO_2MA than that in MA was concluded. By applying the Natural Bond Orbital calculations, the electron inductive, steric, and conjugation effects of NO_2 group were analyzed. According to these calculations, steric, and conjugation effects increases the hydrogen bond strength, while the electron withdrawing effect decreases the strength of the bond.

References

[1] A.H. Lowery, C. George, P.D. Antonio, J. Karle, J. Am. Chem. Soc. 93 (1971) 6399.
[2] R.S. Brown, A.T. Nakashima, R.C. Haddon, J. Am. Chem. Soc. 101 (1979) 3175.
[3] J. Emsley, Structure and Bonding, vol. 2, Springer, Berlin, 1984.
[4] R. Boese, M.Y. Antipin, D. Blaser, K.A. Lyssenko, D. Bläser, K.A. Lyssenko, J. Phys. Chem. B 102 (1998) 8654.
[5] G. Gilli, P. Gilli, J. Mol. Struct. 552 (2000) 1.
[6] S.J. Grabowski, J. Phys. Org. Chem. 16 (2003) 797.
[7] G. Buemi, F. Zuccurello, Chem. Phys. 306 (2004) 115.
[8] S.F. Tayyari, T. Zeegers-Huyskens, J.L. Wood, Spectrochim. Acta 35A (1979) 1265.
[9] S.F. Tayyari, T. Zeegers-Huyskens, J.L. Wood, Spectrochim. Acta 35A (1979) 1289.
[10] T. Chiavassa, P. Verlaque, L. Pizalla, P. Roubin, Spectrochim. Acta 50A (1993) 343.
[11] T. Chiavassa, P. Roubin, L. Pizalla, P. Verlaque, A. Allouche, F. Marinelli, J. Phys. Chem. 96 (1992) 659.
[12] S.F. Tayyari, F. Milani-Nejad, H. Rahemi, Spectrochim. Acta 58A (2002) 1669.
[13] S.F. Tayyari, F. Milani-Nejad, Spectrochim. Acta 56A (2000) 2679.
[14] S.F. Tayyari, S. Salemi, M. Zahedi-Tabrizi, M. Behforouz, J. Mol. Struct. 694 (2004) 91.
[15] A. Nowroozi, S.F. Tayyari, H. Rahemi, Spectrochim. Acta 59A (2003) 1757.
[16] G. Buemi, F. Zuccarello, Electr. J. Theor. Chem. 2 (1997) 302.
[17] J. Emsely, L.Y.Y. Ma, S.C. Nyburg, A.W. Parkins, J. Mol. Struct. 240 (1990) 59.
[18] J. Emsley, L.Y.Y. Ma, P.A. Bates, M. Motevalli, M.B. Hursthouse, J. Chem. Soc., Perkin Trans. 2 (1989) 527.
[19] J. Emsely, L.Y.Y. Ma, S.A. Karaulov, M. Motevalli, M.B. Hursthouse, J. Mol. Struct. 216 (1990) 143.
[20] J. Emsely, N.J. Freeman, P.A. Bates, M.B. Hursthouse, J. Chem. Soc., Perkin Trans. 1 (1988) 297.
[21] E.I. Matrosov, K.K. Babievskii, Izv. Akad. Nauk, SSSR, Ser. Khim. 11 (1972) 2627.
[22] D. Semmingsen, Acta Chem. Scand. Ser. B 31 (1977) 114.
[23] D. Semmingsen, Acta Chem. Scand. Ser. B 28 (1974) 141.
[24] G. A. Taylor, Org. Syntheses, Coll. Vol. 4, p.688.
[25] M.J. Frisch, G.W. Trucks, H.B. Schlegel, G.E. Scuseria, M.A. Robb, J.R. Cheeseman, J.A. Montgomery Jr., T. Vreven, K.N. Kudin, J.C. Burant, J.M. Millam, S.S. Iyengar, J. Tomasi, V. Barone, B. Mennucci, M. Cossi, G. Scalmani, N. Rega, G.A. Petersson, H. Nakatsuji, M. Hada, M. Ehara, K. Toyota, R. Fukuda, J. Hasegawa, M.

Ishida, T. Nakajima, Y. Honda, O. Kitao, H. Nakai, M. Klene, X. Li, J.E. Knox, H.P. Hratchian, J.B. Cross, C. Adamo, J. Jaramillo, R. Gomperts, R.E. Stratmann, O. Yazyev, A.J. Austin, R. Cammi, C. Pomelli, J.W. Ochterski, P.Y. Ayala, K. Morokuma, G.A. Voth, P. Salvador, J.J. Dannenberg, V.G. Zakrzewski, S. Dapprich, A.D. Daniels, M.C. Strain, O. Farkas, D.K. Malick, A.D. Rabuck, K. Raghavachari, J.B. Foresman, J.V. Ortiz, Q. Cui, A.G. Baboul, S. Clifford, J. Cioslowski, B.B. Stefanov, G. Liu, A. Liashenko, P. Piskorz, I. Komaromi, R.L. Martin, D.J. Fox, T. Keith, M.A. Al-Laham, C.Y. Peng, A. Nanayakkara, M. Challacombe, P.M.W. Gill, B. Johnson, W. Chen, M.W. Wong, C. Gonzalez, J.A. Pople, GAUSSIAN03, Revision B.05, Gaussian, Inc., Pittsburgh PA, 2003.

[26] NBO 5.0, J.K. Badenhoop, A.E. Reed, J.E. Carpenter, J.A. Bohmann, C.M. Morales, F. Weinhold, E.D. Glendening, Theoretical Chemistry Institute, University of Wisconsin, Madison, 2001.

[27] A.D. Becke, J. Chem. Phys. 98 (1993) 5648.

[28] C. Lee, W. Yang, R.G. Parr, Phys. Rev. B 37 (1988) 785.

[29] K.W. Wiberg, Tetrahedron 24 (1968) 1083.

[30] J.K. Badenhoop, F. Weinhold, J. Chem. Phys. 107 (1997) 5406.

[31] J.K. Badenhoop, F. Weinhold, Int. J. Quantum Chem. 72 (1999) 269.

[32] A.E. Reed, L.A. Curtiss, F. Weinhold, Chem. Rev. 88 (1988) 899.

[33] Z. Smith, E.B. Wilson, R.W. Durest, Spectrochim. Acta 39A (1983) 117.

[34] W. Caminati, J. Chem. Soc., Faraday Trans., 2 78 (1982) 825.

[35] V. Bertolasi, P. Gilli, V. Ferreti, G. Gilli, J. Am. Chem. Soc. 113 (1991) 4917.

[36] C.A. Télles, E. Hollauer, M.I. Pais da Silva, M.A. Momdragón, I. Haiduc, M. Curtui, Spectrochim. Acta 57A (2001) 1149.

[37] N.B. Colthup, L.H. Daly, S.E. Wiberley, Introduction to Infrared and Raman Spectroscopy, Academic, 1964.

[38] C. Passingham, P.J. Hendra, C. Hodges, H.A. Willis, Spectrochim. Acta 47A (1991) 1235.

[39] R.D. Kross, V.A. Fassel, J. Am. Chem. Soc. 78 (1956) 4225.